DOI 10.1007/s10812-017-0459-6
Journal of Applied Spectroscopy, Vol. 84, No. 2, May, 2017 (Russian Original Vol. 84, No. 2, March–April, 2017)

CATHODOLUMINESCENCE OF Y_2O_3:Eu THIN FILMS OBTAINED BY RF SPUTTERING

O. M. Bordun,* I. O. Bordun, and I. Yo. Kukharskyy

UDC 535.37;621.315.612;539.216.2

The cathodoluminescent (CL) properties of Y_2O_3:Eu thin films obtained by RF magnetron sputtering were investigated. The number of Eu^{3+} ions in C_2 states of lower symmetry was hypothesized to be greater in the film bulk than on the surface based on studies of the CL spectral intensity as a function of the exciting-electron energy and current density. It was shown that film structural defects and the excitation conditions influenced the kinetic characteristics of the red emission of Y_2O_3:Eu at 612 nm that was due to the electric dipole transition $^5D_0 - ^7F_2$.

Keywords: *yttrium oxide, cathodoluminescence, thin film.*

Introduction. Luminescent materials that are used to fabricate displays, scintillators, and information recording and visualization devices are especially significant optoelectronic materials. Cubic yttrium oxide activated by rare-earth metal ions is a common luminophore crystalline matrix [1–5]. The phosphor Y_2O_3:Eu with red emission is the most well studied micron-sized luminophore. Results from previous studies of this material can be used as supporting information to analyze the luminescence characteristics and mechanism during investigations of size effects on the emission efficiency of submicron luminophores [6]. Therefore, we used local cathodoluminescence (CL) (luminescence excited by an electron beam), which has several advantages over traditional optical methods. This method typically is highly sensitive to changes in the material electronic structure (dopants and structural defects) and makes it possible to study changes in the luminescent properties of structures and materials to a depth of 10–20 nm to several micrometers. Furthermore, the high luminescence excitation energy enables optical transitions that require energies >6 eV for excitation (from the vacuum UV region) to be studied. This method also allows energy-transfer processes between high-energy states and the electronic structure of defects that are channels for nonradiative recombination to be investigated. It is noteworthy that a whole series of methods have been used to prepare Y_2O_3 films. Therefore, the films differed in optical and luminescent properties as a result of their different qualities.

Herein, the CL properties of Y_2O_3:Eu thin films obtained by RF ion-plasma sputtering were studied. The method deposits the most uniform semiconducting and dielectric films [7, 8].

Experimental. Y_2O_3:Eu thin films (0.2–1.0 μm) were obtained by RF ion-plasma sputtering in 100% O_2 or 100% Ar atmosphere using the magnetic field from external solenoids to compress and also ionize a plasma column on *v*-SiO_2 fused quartz substrates. The starting materials were Y_2O_3 (ItO-I grade) and Eu_2O_3 (high purity). The activator concentrations were 2.5 and 5.0 mol%. Deposited films were heat treated at 950–1050°C in air.

X-ray phase analysis is one of the most reliable methods for determining the composition and structure of materials. Figure 1 shows x-ray diffraction patterns of freshly prepared Y_2O_3:Eu thin films and those annealed in air. The diffraction pattern contained a broad band near $2\Theta = 28–31^o$ that was due to reflection from the (222) plane of cubic Y_2O_3 ($2\Theta = 29.18^o$ for the ordered structure). The reflection maximum shifted to higher 2Θ angles and became asymmetric if the sputtering atmosphere was changed from Ar to O_2. The reason for the shift was most probably a decrease of the interplanar distances in Y_2O_3. The influence of the atmosphere on the properties of Y_2O_3 films was discussed in more detail before [9]. The intensities of the diffraction maxima increased sharply after annealing and became considerably narrower (Fig. 1b). The results indicated that cubic Y_2O_3 became ordered during annealing at 950–1050°C.

*To whom correspondence should be addressed.

Ivan Franko L′viv National University, 50 Dragomanov Str., L′viv, 79005, Ukraine; e-mail: bordun@electronics.lnu.edu.ua. Translated from Zhurnal Prikladnoi Spektroskopii, Vol. 84, No. 2, pp. 226–232, March–April, 2017. Original article submitted February 19, 2016.

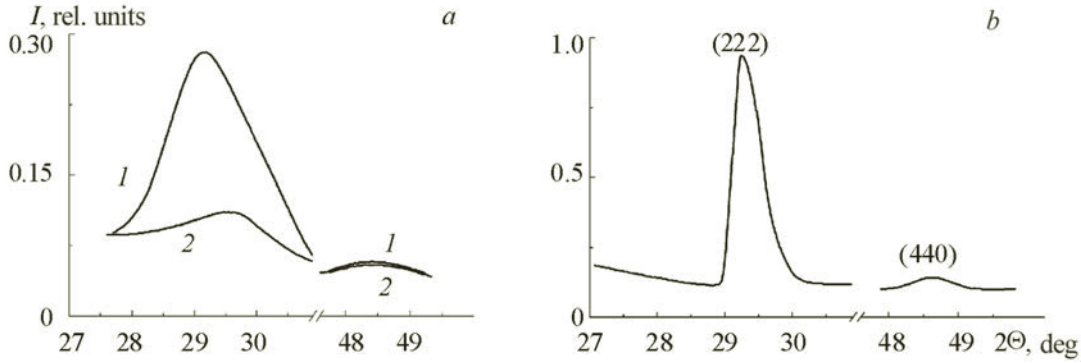

Fig. 1. X-ray diffraction patterns of freshly prepared Y_2O_3:Eu thin films obtained in Ar (1) and O_2 (2) atmospheres (a) and of a film prepared in Ar atmosphere that was annealed at 1000°C in air (b).

The width of diffraction peaks is known to depend on the size of the coherent scattering regions (crystallite size). The crystallite size d is determined from the well-known Debye–Scherrer equation [10] for the broadening of x-ray diffraction peaks: $d = 0.94\lambda/(\beta \cos \Theta)$, where $\lambda = 0.15418$ nm is the wavelength of CuK_α-radiation; β, the peak width at half height; and Θ, the diffraction angle. The sizes of the crystallites forming the Y_2O_3:Eu thin films as a function of the preparation conditions were estimated based on the results. In particular, it was found that the crystallite sizes d = 5.5–6.0 nm for RF sputtering in an Ar atmosphere; 6.5–7.0 nm, in O_2. Annealing increased the crystallite size because of their growth and sintering. For example, the crystallite size reached d = 28.0–32.0 nm for annealing temperature 1000°C.

The CL properties were studied using pulsed-electron excitation. Spectra were recorded on an apparatus assembled around an SF-4A spectrophotometer (Russia) using an FEU-79 photomultiplier. Decay curves were recorded using the FEU-79 and a C1-117 electronic oscilloscope (Belarus) connected to an IBM/PC.

Results and Discussion. Figure 2 shows characteristic CL spectra of the obtained Y_2O_3:Eu films at various exciting-electron energies and current densities. Narrow bands due to intrasystem transitions between electronic states of the activator Eu^{3+} appeared in luminescence spectra of the films. The wavelength of the emission maximum λ_{max} = 612 nm agreed with the red color. Figure 2 shows all observed electronic transitions $^5D_0$–^7F_J for Eu^{3+}. They include allowed magnetic dipole transitions $^5D_0$–$^7F_1$ (for Eu^{3+} at C_2 and C_{3i} sites of the Y_2O_3 lattice) and allowed electric dipole transitions $^5D_0$–$^7F_2$ (for Eu^{3+} only at C_2 sites). The unit cell of cubic Y_2O_3 contains 32 Y^{3+} ions that can be replaced by other rare-earth ions. The Y^{3+} ions occupy 8 positions with a center of symmetry (C_{3i} symmetry) and 24 positions of lower symmetry (C_2) [11, 12]. Thus, the Eu^{3+} ions can occupy one of two inequivalent positions, leading to differences in the luminescence spectra. Considering that the ionic radii of Y^{3+} and Eu^{3+} are very similar (0.90 and 0.94 Å), Y_2O_3 retains the cubic crystalline lattice with slight changes upon activation by Eu^{3+} [13]. The so-called asymmetry ratio I_{612}/I_{596} of intensity maxima near 612 and 596 nm is often used to describe Y_2O_3:Eu luminescence spectra. This corresponds to the ratio of the numbers of Eu^{3+} in states of local symmetry, N_{C2}/N_{C3i} [6, 13–16]. The luminescence band at 612 nm is due to the electric dipole transition $^5D_0$–$^7F_2$, which is very sensitive to the closest environment of the emitting Eu^{3+} ion. The band with a maximum at 596 nm corresponds to magnetic dipole transition $^5D_0$–$^7F_1$, which is insensitive to the closest environment [13, 16–18]. The ratio of intensities I_{612}/I_{596} is used to estimate N_{C2}/N_{C3i} [6, 15, 17, 19] and to analyze the structural quality of Y_2O_3:Eu^{3+}.

The ratio N_{C2}/N_{C3i} for Y^{3+} in an ideal Y_2O_3 matrix at equilibrium is 3:1. A similar result should be obtained if the Eu^{3+} ions are uniformly substituted for Y^{3+}. However, this ratio in Y_2O_3:Eu thin films was much greater and also depended on the exciting-electron current density and energy. For example, increasing the current density from $6.6\cdot10^{-3}$ to $12.1\cdot10^{-3}$ A/m^2 at exciting-electron energy 6 keV increased this ratio from 8.5 to 9.25 (Fig. 2b). Increasing the exciting-electron energy from 5.5 to 6.0 keV at current density $5\cdot10^{-3}$ A/m^2 increased this ratio from 10.4 to 14.0 (Fig. 2a). It is noteworthy that similar amplitude ratios I_{612}/I_{596} = 8–10 were obtained before [6] during a study of the photoluminescence of powdered Y_2O_3:Eu materials of various dispersions that were synthesized by the sol-gel method.

Our results indicated that Eu^{3+} at C_2 sites contributed more to the emission than those at C_{3i} sites if the number of bombarding electrons and their penetration depth were increased. If the Eu^{3+} replaced Y^{3+} uniformly in the Y_2O_3 lattice, then changing the electron-beam current density should not affect I_{612}/I_{596}. However, several deviations were observed and most likely were indicative of the formation of heterogeneous solutions of Y and Eu oxides in the Y_2O_3:Eu thin film during its deposition.

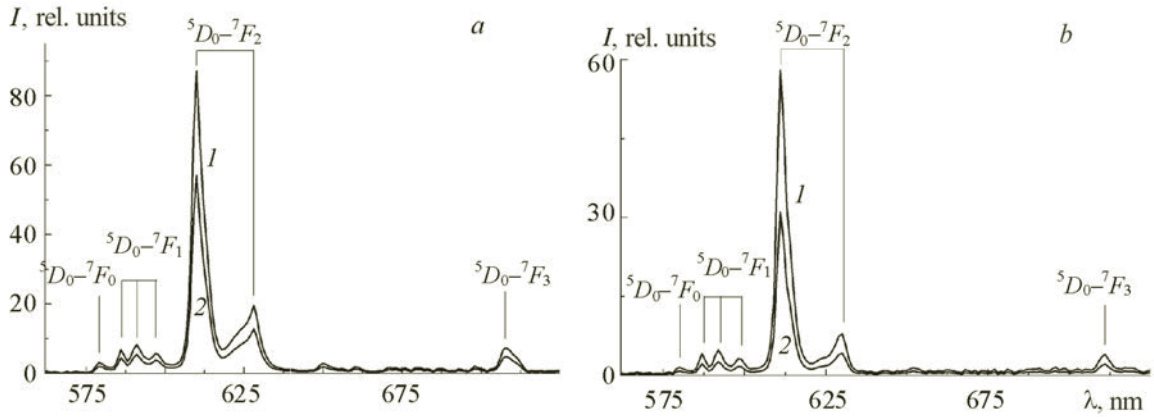

Fig. 2. CL spectra of Y_2O_3:Eu thin films with various exciting-electron energies (a) and current densities (b); activator concentration 5%, sputtering atmosphere 100% Ar (a) and 100% O_2 (b); exciting-electron pulse parameters: pulse length $5\cdot10^{-4}$ s, pause between pulses 0.1 s; electron-beam current density $j = 5\cdot10^{-2}$ A/m^2, exciting-electron energy 5.0 (1) and 4.5 keV (2) (a); exciting-electron energy 6 keV, electron-beam current density $12\cdot10^{-3}$ (1) and $6.5\cdot10^{-3}$ A/m^2 (2) (b).

Increasing the exciting-electron energy and their penetration depth showed that the number of Eu^{3+} at C_{3i} sites predominated on the film surface relative to the bulk. The increased relative number of Eu^{3+} at C_2 sites in the film bulk deposited in an Ar atmosphere (Fig. 2a) was caused by local symmetry lowering of the Eu^{3+} environment by O^{2-} ions. The local symmetry of Eu^{3+} primarily near the surface was increased because the films were annealed in air.

Figure 3 shows the CL intensity as a function of exciting-electron energy at various pulse lengths. It can be seen that the CL intensity increased as the excitation energy increased. This path was followed by Y_2O_3:Eu films up to a certain E_{ex} value that was determined by the film thickness. In particular, this energy was ~5.0 keV for a Y_2O_3:Eu film 0.20 μm thick (Fig. 3a). After this, the CL intensity decreased slightly and began to increase again after reaching excitation energy 5.5 keV. The path of the function was due to the passage of the exciting beam through the film and into the substrate upon reaching an energy of 5.0 keV. As a result, the number of bombarding electrons of energies >5 keV that interacted with the film decreased whereas the number interacting with the substrate increased. This caused the CL intensity at 5.0–5.5 keV to decrease. The quantity 5.5 keV was not intrinsic to Y_2O_3:Eu but was related to the thickness of the deposited film [20]. The electron energy at which the emission intensity maximum occurred decreased (increased) if the film thickness was decreased (increased). It is noteworthy that the CL intensity was a complicated function of the excitation energy and radiation dose. Because the measurements were made with a fixed number of bombarding electrons, the subsequent CL intensity increase at excitation energies >5.5 keV could be explained only by the increased energy of the bombarding electrons. The aforementioned CL intensity minimum was not observed for an exciting pulse length of $4\cdot10^{-4}$ s, i.e., at the minimum radiation dose in this study. This approach could also be used to explain the rather sharp CL intensity increase upon increasing the exciting-beam current (Fig. 3b). An analysis of the CL excitation mechanism of the Y_2O_3:Eu luminophore must assume that the CL intensity should increase in direct proportion to an increase of the concentration of bombarding particles. The intensity increase should slow and become saturated upon reaching a certain critical excitation current because all possible emission centers begin to participate in the CL process. However, the experimental function (Fig. 3) differed slightly from direct proportionality. The CL intensity increased slightly slower. This led to the conclusion that the excitation energy in this cathodoluminophore was not fully transferred from the exciting electron to an emission center, i.e., a part of the energy went to nonradiative processes that could be caused by film structural defects. The path of this function became closer to directly proportional as the excitation time, i.e., the radiation dose, was increased.

The order of the CL decay kinetics in Y_2O_3:Eu films for emission at λ_{max} = 612 nm was analyzed in order to study the energy-transfer mechanism of rare-earth activators in Y_2O_3 films. Figure 4 shows characteristic kinetics of the studied films. It was found that the luminescence decay kinetics in Y_2O_3:Eu films at various radiation energies and doses were approximated well by single-exponential functions. The results indicated that the decay time constant changed depending on the film sputtering atmosphere, activator concentration, and excitation pulse length. In particular, Y_2O_3:Eu films deposited in an Ar atmosphere with activator concentration 5 mol% showed brighter luminescence than films with 2.5 mol% of activator.

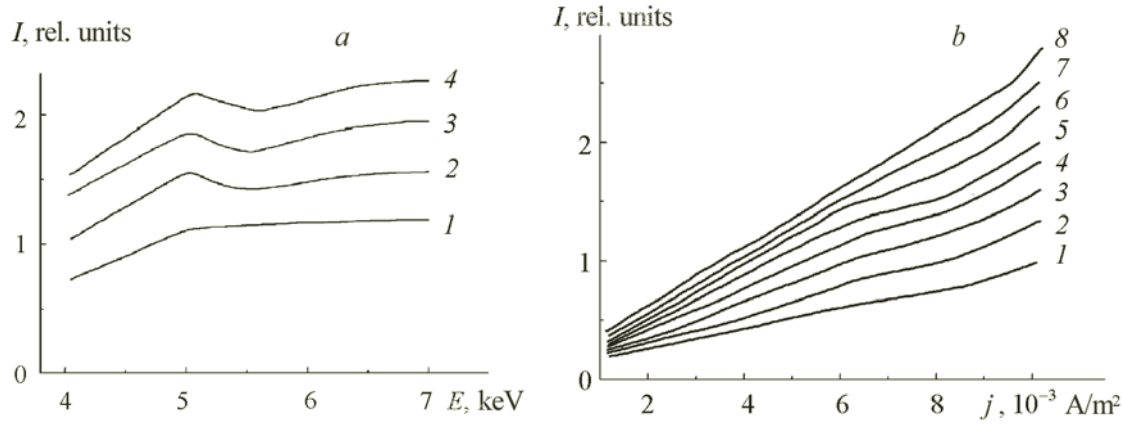

Fig. 3. CL intensity of Y_2O_3:Eu thin films as a function of exciting-electron energy (a) and current density (b); activator concentration 2.5 (a) and 5% (b), sputtering atmosphere 100% Ar; exciting-electron pulse parameters: electron-beam current density 10^{-2} A/m^2, excitation pulse length $4\cdot10^{-4}$ (1), $6\cdot10^{-4}$ (2), $8\cdot10^{-4}$ (3), and 10^{-3} s (4) (a); exciting-electron energy 2.5 keV, pulse length $3\cdot10^{-4}$ (1), $4\cdot10^{-4}$ (2), $5\cdot10^{-4}$ (3), $6\cdot10^{-4}$ (4), $7\cdot10^{-4}$ (5), $8\cdot10^{-4}$ (6), $9\cdot10^{-4}$ (7), and 10^{-3} s (8); pause between pulses 0.1 s.

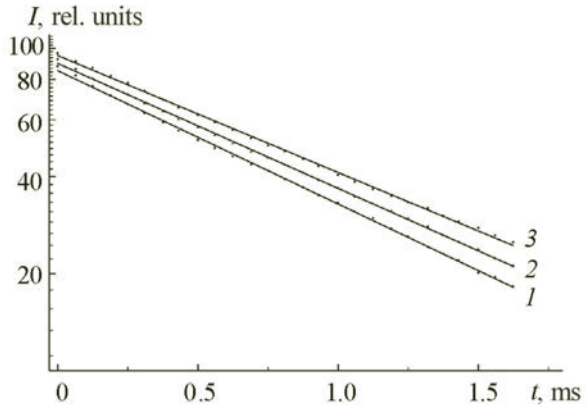

Fig. 4. CL decay kinetics of Y_2O_3:Eu thin films as a function of exciting-electron energy; activator concentration 5%, sputtering atmosphere 100% O_2; exciting-electron pulse parameters: pulse length $5\cdot10^{-4}$ s, pause between pulses 0.1 s, electron-beam current density 10^{-2} A/m^2, bombarding-electron energy 4.0 (1), 5.5 (2), and 7.0 keV (3).

The decay time constant for the first films was greater than that for the second (Table 1). However, the decay constants for both films at low excitation lengths ($4\cdot10^{-4}$ s) were greater than that at long CL excitation lengths [$(6–9)\cdot10^{-4}$ s]. This could be explained by the fact that film shallow layers were more heterogeneous than those in the bulk. Therefore, these defects contributed to the emission kinetics and increased decay constant τ after the exciting-electron pulse ended. This was more evident at the weaker emission intensities that were observed at smaller radiation doses, i.e., shorter excitation pulse lengths.

Table 1 shows that the CL decay time constant in Y_2O_3:Eu thin films for emission at 612 nm was $(1.8–4.1)\cdot10^{-3}$ s depending on the film structure quality and activator concentration. According to theoretical calculations of electric dipole, magnetic dipole, and electric quadrupole transitions in lanthanides: $\tau_{el} \sim 10^{-4}$ s, $\tau_{mag} \sim 0.5\cdot10^{-2}$ s; and $\tau_q \sim 2$ s [21]. A comparison of our values with results based on the emission spectrum (Fig. 1) showed that an electric dipole transition was involved and that Eu^{3+} emitting at 612 nm were situated at Y_2O_3 crystal-lattice sites with C_2 point symmetry. It is also noteworthy that the obtained time constants τ agreed well with those from previous investigations of luminescence decay in various Y_2O_3:Eu specimens [22–26]. Thus, a value of 1.3 ms was obtained by determining the decay time of the $^5D_0$–$^7F_2$ transition in Y_2O_3:Eu ceramics with 10-nm crystallites [22]. The decay time constants fell in the range 2.0–3.7 ms

TABLE 1. CL Decay Time Constant in Y_2O_3:Eu Thin Films for Emission at 612 nm and Various Sputtering Atmospheres, Activator Concentrations, and Excitation Times with U_{ex} = 4.5 keV

Sputtering atmosphere	C_{activ}, mol%	t_{ex}, 10^{-4} s	τ, 10^{-3} s
Argon 100%	2.5	4	3.7
		6	2.2
		9	2.2
Argon 100%	5.0	4	4.1
		6	3.4
		9	3.3
Oxygen 100%	5.0	4	2.0
		6	1.9
		9	1.8

for Y_2O_3:Eu single crystals [23]. The lifetime of Y_2O_3:Eu nanophosphors (5–7 nm) with activator concentration 2.4 mol% was 3.08 ms; for activator concentration 5.2 mol%, 2.40 ms. The decay constant of the 612-nm emission was less for single crystals, e.g., τ = 1.07 ms for activator concentration 3.5 mol% and 1.02 ms for 5.2 mol%. According to the literature [25], τ ≈ 4 ms in Y_2O_3:Eu nanocrystals whereas τ = 1.90 and 1.72 ms for activator concentrations 3 and 8% in Y_2O_3:Eu single crystals [24]. The studies showed that such differences in the emission decay time constant of Y_2O_3:Eu at 612 nm that was due to electric dipole transition $^5D_0$–$^7F_2$ were caused by τ being a complicated function that was determined by the preparation method and conditions, radiation mode and dose, crystallite size, structure quality, and activator concentration.

Conclusions. Thin films of Y_2O_3:Eu with crystallite sizes 5.5–7.0 nm were prepared by RF ion-plasma sputtering in Ar and O_2 atmospheres. Annealing in air ordered the structure and increased the crystallite sizes to 28.0–32.0 nm. Studies of the CL spectra indicated that heterogeneous solutions of Y and Eu oxides may have formed in the Y_2O_3:Eu thin films and that the number of Eu^{3+} at sites of lower symmetry C_2 was increased in the film bulk relative to the surface. Energy transfer from electrons absorbed by the film to activator centers improved if the radiation dose was increased, i.e., the exciting-pulse length increased from $3\cdot10^{-4}$ s to 10^{-3} s. The luminescence decay kinetics showed that film structural defects affected the energy-transfer mechanism of absorbed electrons to activator ions. It was hypothesized that shallow layers were structurally more heterogeneous than those in the bulk.

REFERENCES

1. K. Mishra, Y. Dwivedi, and S. B. Rai, *Appl. Phys. B: Lasers Opt.*, **106**, No. 1, 101–105 (2012).
2. H. J. Lee, K. P. Kim, G. Y. Hong, and J. S. Yoo, *J. Lumin.*, **130**, No. 6, 941–946 (2010).
3. Q. Dai, M. E. Foley, C. J. Breshike, A. Lita, and G. F. Strouse, *J. Am. Chem. Soc.*, **133**, No. 39, 15475–15486 (2011).
4. G. Ju, Y. Hu, L. Chen, X. Wang, Z. Mu, H. Wu, and F. Kang, *J. Lumin.*, **132**, No. 8, 1853–1859 (2012).
5. C. Shanga, X. Shang, Y. Qu, and M. Li, *Chem. Phys. Lett.*, **501**, 480–484 (2011).
6. T. A. Pomelova, V. V. Bakovets, I. V. Korol′kov, O. V. Antonova, and I. P. Dolgovesova, *Fiz. Tverd. Tela*, **56**, No. 12, 2410–2419 (2014).
7. L. I. Maissel and R. Glang (Eds.), *Handbook of Thin Film Technology*, McGraw-Hill, New York (1970) [Russian translation, Sov. Radio, Moscow (1977)].
8. E. V. Berlin and L. A. Seidman, *Ion-Plasma Processes in Thin-film Technology* [in Russian], Tekhnosfera, Moscow (2010).
9. O. M. Bordun, I. O. Bordun, and I. I. Kukharskii, *Zh. Prikl. Spektrosk.*, **82**, No. 3, 380–385 (2015) [O. M. Bordun, I. O. Bordun, and I. Yo. Kukharskyy, *J. Appl. Spectrosc.*, **82**, 390–395 (2015)].
10. V. D. Andreeva, E. V. Novikov, I. K. Boricheva, and A. B. Speshilova, *Special Methods in X-ray Diffraction and Electron-Microscopy Studies of Materials* [in Russian], Izd. Politekh. Univ., St. Petersburg (2008).
11. N. C. Chang and J. B. Gruber, *J. Chem. Phys.*, **41**, No. 10, 3227–3234 (1964).
12. G. Blasse and B. C. Grabmaier, *Luminescent Materials*, Springer-Verlag, Berlin (1994).
13. S. Som, S. K. Sharma, and S. P. Lochab, *Mater. Res. Bull.*, **48**, No. 2, 844–851 (2013).

14. H. S. Yoo, W. B. Im, S. W. Kim, B. H. Kwon, and D. Y. Jeon, *J. Lumin.*, **130**, No. 1, 153–156 (2010).
15. R. M. Krsmanovic, Z. Antic, M. G. Nikolic, M. Mitric, and M. D. Dramicanin, *Ceram. Int.*, **37**, No. 2, 525–531 (2011).
16. F. C. Romo, A. G. Murillo, D. L. Torres, N. C. Castro, V. H. Romero, E. Rosa, V. G. Febles, and M. G. Hernandez, *Opt. Mater.*, **32**, No. 11, 1471–1479 (2010).
17. W.-N. Wang, W. Widiyastuti, T. Ogi, I. W. Lenggoro, and K. Okuyama, *Chem. Mater.*, **19**, No. 7, 1723–1730 (2007).
18. G. S. Gowd, M. K. Patra, S. Songara, A. Shukla, M. Mathew, S. R. Vadera, and N. Kumar, *J. Lumin.*, **132**, No. 8, 2023–2029 (2012).
19. R. Srinivasan, N. R. Yogamalar, J. Elanchezhiyan, R. J. Joseyphus, and A. C. Bose, *J. Alloys Compd.*, **496**, Nos. 1–2, 472–477 (2010).
20. O. M. Bordun, E. V. Dovga, and I. I. Kukharskii, *Zh. Prikl. Spektrosk.*, **78**, No. 4, 644–648 (2011) [O. M. Bordun, I. V. Dovga, and I. Yo. Kukharskyy, *J. Appl. Spectrosc.*, **78**, 605–609 (2011)].
21. D. T. Sviridov and Yu. F. Smirnov, *Theory of Optical Spectra of Transition Metal Ions* [in Russian], Nauka, Moscow (1977).
22. U. Herr, H. Kaps, and A. Konrad, *Solid State Phenom.*, **94**, 85–94 (2003).
23. R. Schmechel, M. Kennedy, H. von Seggern, H. Winkler, M. Kolbe, R. A. Fischer, L. Xaomao, A. Benker, M. Winterer, and H. Hahn, *J. Appl. Phys.*, **89**, No. 3, 1679–1686 (2001).
24. H. Kaps, M. L. Arefin, U. Herr, and H. Paul, *Solid State Phenom.*, **128**, 165–172 (2007).
25. P. K. Sharma, R. K. Dutta, and A. C. Pandey, *Adv. Mater. Lett.*, **2**, No. 4, 285–289 (2011).
26. C. Hang, Z. Pei-Fen, Z. Hong-Yang, L. Hong-Dong, and C. Qi-Liang, *Chin. Phys. B*, **23**, No. 5, 057801 (1–6) (2014).